Harmful Algae 129 (2023) 102523

Contents lists available at ScienceDirect

Harmful Algae

journal homepage: www.elsevier.com/locate/hal

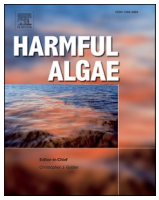

Where does floating *Sargassum* in the East China Sea come from?

Lin Qi [a,b,*], Peng Cheng [c], Menghua Wang [a], Chuanmin Hu [d], Yuyuan Xie [d], Keyu Mao [d]

[a] NOAA Center for Satellite Applications and Research, College Park, MD 20740, USA
[b] Global Science & Technology Inc., Greenbelt, MD 20770, USA
[c] State Key Laboratory of Marine Environmental Science, Xiamen University, Xiamen 361102, China
[d] College of Marine Science, University of South Florida, St. Petersburg, FL 33701, USA

ARTICLE INFO

Edited by: Dr Po Teen Lim

Keywords:
Sargassum horneri
East China Sea
Yellow Sea
Bohai Sea
Aquaculture
Remote sensing
Sentinel-2
MSI
VIIRS
MODIS
ROMS
Global warming

ABSTRACT

Floating macroalgae of *Sargassum horneri* (*S. horneri*) in the East China Sea (ECS) has increased in recent years, with ocean warming being one of the driving factors. Yet their possible origins, based on a literature review, are unclear. Here, using multi-sensor high-resolution remote sensing data and numerical experiments for the period of 2015–2023, we show two possible origins of the ECS floating *S. horneri*, one being local near the Zhejiang coast with initiation in January–February and the other being remote (> 800 km from the first) in the Bohai Sea with initiation in June–November. While their drifting pathways are revealed in the sequential remote sensing imagery, numerical experiments suggest that *S. horneri* from the remote origin (Bohai Sea) can hardly meander through the strong Yangtze River frontal zone, which may serve as a "wall" to prevent trespassing of surface floating seaweed to the south of the frontal zone, where *S. horneri* has a local origin.

Plain language summary: Sargassum horneri (*S. horneri*) is a brown macroalgae (seaweed) abundant in surface waters of the East China Sea (ECS), which can serve as a moving habitat, but can also cause major beaching events and environmental problems. Knowledge of its origins is important to help implement mitigation strategies and understand possible ecological impacts along its drifting pathways. Using high-resolution remote sensing images and numerical experiments, we track floating *S. horneri* in space and time between 2015 and 2023. Two possible origins are identified, one being far away from the ECS and the other being local, both of which are known to have benthic *S. horneri*. The study also reveals how *S. horneri* are transported from their source regions resulting in large-scale distributions previously observed in medium-resolution satellite imagery.

1. Introduction

In recent years, large amounts of *Sargassum horneri* (*S. horneri*) macroalgae with a multi-year cumulative footprint of ~500,000 km^2 and maximum mean monthly biomass of ~607,000t reported in surface waters of the East China Sea (ECS, Figs. 1 and 2, Qi et al., 2022a), with an apparent increasing trend (Qi et al., 2022a). *S. horneri* is commonly found in intertidal zones and shallow subtidal areas in the western Pacific Ocean, including coastal regions in Japan, China, and Korea (Umezaki, 1984). It can grow up to several meters in length and form dense clusters that are often referred to as "marine forests." *S. horneri* plays a crucial role in coastal ecosystems by providing habitat and food for a variety of marine organisms (Komatsu et al., 2014; Rosenblatt et al., 2022).

Occasionally, *S. horneri* detach from the seafloor due to storms or strong ocean currents, and then continue its life cycle while drifting on the ocean surface (Fig. 1). The detached seaweed can form floating mats that are transported long distances by ocean currents and grow rapidly under suitable growth conditions such as more light and warmer surface ocean waters. The resulting blooms, often called 'golden tides' in the ECS and the adjacent Yellow Sea (YS), can cause large beaching events and many negative environmental impacts (Chen et al., 2019; Xiao et al., 2020; Xing et al., 2017) similar to the recurrent blooms of the green macroalgae *Ulva prolifera* in the YS (Hu et al., 2023a).

Scattered *S. horneri* mats in surface waters of the ECS were first reported by Komatsu et al. (2007) from in situ surveys, while the first *S. horneri* mats captured in satellite imagery were in 2000 (Qi et al., 2022a). Large-scale *S. horneri* blooms in the ECS did not occur until 2015 (Qi et al., 2017), with major blooms reported in 2017 and subsequent years (Qi et al., 2022a; Xing et al., 2017; Wang et al., 2023). Since then, more research has been conducted to understand bloom patterns in both space and time. For example, the recent expansions of *S. horneri* blooms have been attributed primarily to ocean warming as temperature is a

* Corresponding author at: NOAA Center for Satellite Applications and Research, College Park, MD 20740, USA.
E-mail address: lin.qi@noaa.gov (L. Qi).

https://doi.org/10.1016/j.hal.2023.102523
Received 15 June 2023; Received in revised form 25 September 2023; Accepted 4 October 2023
Available online 10 October 2023

Nomenclature

R_{rc}	Rayleigh-corrected reflectance (dimensionless), wavelength dependent
DL	deep learning, one type of machine learning
AFAI	Alternative Floating Algae Index, a scalar quantity derived from a linear combination of reflectance at three bands (R_{b1}, R_{b2}, R_{b3})
FRGB	False Red-Green-Blue composite, where the green channel uses a NIR band instead of a green band in the RGB composite.
OCView	Ocean Color Viewer, an online tool developed by NOAA to visualize ocean color imagery in near-real-time (https://www.star.nesdis.noaa.gov/socd/mecb/color/)
TOA	Top of Atmosphere
CZI	Coastal Zone Imager onboard the HY-1C (2018–present) and HY-1D (2020–present) satellites
GF	Gao-Fen (high resolution in English translation), a series of Chinese satellite missions starting 2013 to map Earth's surface
GOCI	Geostationary Ocean Color Imager, which is on the Korean Communication, Ocean, and meteorological Satellite (2011–2021)
HJ	Huan-Jing (environment in English translation), Chinese satellite missions starting 2008 to map Earth's surface with high-resolution sensors (3–100m)
Landsat	a series of Earth-observing satellite missions since 1972, with most missions equipped with multi-band sensors, 30m resolution
MSI	MultiSpectral Instrument, which is on the Sentinel-2A (2015–present) and Sentinel-2B (2017–present) satellites, 10–60m resolution
MODIS	Moderate Resolution Imaging Spectroradiometer, which is on the Terra (1999–present) and Aqua (2002–present) satellites, 250, 500, and 1000m resolution
VIIRS	Visible Infrared Imaging Radiometer Suite, which is on the Suomi National Polar-orbiting Partnership (2011–present), NOAA-20 (2017–present), and NOAA-21 (2022–present) satellites, 375 and 750m resolution
ECMWF	European Center for Medium-range Weather Forecasts
HYCOM	the Hybrid Coordinate Ocean Model (Bleck and Boudra, 1981)
POM	Princeton Ocean Model (Mellor, 2003)
ROMS	Regional Ocean Modeling System (Shchepetkin and McWilliams, 2005)
LTRANS	Larval TRANSport Lagrangian model (North et al., 2008)

crucial factor affecting seaweed growth (Choi et al., 2007; Qi et al., 2022a; Shin et al., 2022; Yu et al., 2019). However, there is still no clear understanding on the blooms' possible origins despite the numerous research results published in the recent literature (e.g., Byeon et al., 2019; Li et al., 2020; Yuan et al., 2022, also see literature review below).

The objective of this research is to determine the possible origins of the floating *S. horneri* in the ECS. To achieve this, we first reviewed the literature to summarize the findings from relevant publications. Next, we analyzed high-resolution satellite images to track the temporal evolutions of floating *S. horneri* in each year between 2015 and 2023. Finally, we conducted numerical experiments to simulate the *S. horneri* drifting pathways with both realistic initialization (based on satellite observations) and hypothetical initialization (based on logical inferences). While the satellite images enabled us to observe the distinct distribution patterns of *S. horneri* and track their changes over time, the numerical experiments explained how *S. horneri* was transported over time to result in the observed distribution patterns.

2. Data and method

2.1. Literature review

The literature database available at the Web of Science (https://webofscience.com) was searched in May 2023 with the keyword combination of "*Sargassum*" and "East China Sea," resulting in 112 references. Of these references, those not directly relevant to *Sargassum* origins were excluded. The remaining references were further searched through Google Scholar to obtain additional papers that cited these references. Finally, only those papers that investigated the possible origins of *S. horneri* were compiled and studied.

2.2. Remote sensing

2.2.1. Satellite data

Satellite remote sensing was used to detect and track floating *S. horneri* in the study region (Figs. 1 and 2). Two types of satellite images were used for different purposes. While the medium-resolution images collected by the Visible Infrared Imaging Radiometer Suite (VIIRS, 375 and 750 m resolutions, 2011–present) or the Moderate Resolution Imaging Spectroradiometer (MODIS, 250, 500, and 1000 m, 1999–present) provide daily observations to enable the detection of relatively large image features and calculation of long-term statistics, high-resolution images collected by the MultiSpectral Instrument (MSI, 10–60 m, 2015–present on Sentinel-2A and 2017–present on Sentinel-2B) can detect much finer image features, thus they are more suitable to track early stages of bloom occurrence and the possible origins of *S. horneri*. With two satellites in orbit after March 2017, MSI provided 5-day revisits at a local time of ~10:30 am.

In this study, the MSI top-of-atmosphere (TOA) reflectance data were provided by the European Space Agency through Google Earth Engine (https://developers.google.com/earth-engine/datasets/catalog/COPERNICUS_S2_HARMONIZED). More than 11,000 tiles of MSI images covering the YS and ECS were downloaded and analyzed to track the origins of *S. horneri*. In addition, VIIRS Rayleigh-corrected reflectance (R_{rc}) data on 6 April 2021 were provided by the U.S. National Oceanic and Atmospheric Administration (NOAA) Ocean Color Science Team, which were analyzed to validate the results from the numerical experiments (see below).

2.2.2. Sargassum feature extraction from satellite images

A deep learning (DL) model, based on the Res-UNet architecture (Ronneberger et al., 2015; Zhang et al., 2018), was employed to detect and extract *S. horneri* features from MSI images based on each pixel's reflectance spectral shape and its spatial context (Qi et al., 2023). Res-UNet is an enhanced iteration of the U-Net model, initially introduced by Ronneberger et al. (2015). Zhang et al. (2018) further refined and adapted this model specifically to extract road information from satellite images. Due to its effectiveness in accurately identifying and extracting objects, Res-UNet has also been used to extract floating algae features from satellite images (Hu et al., 2023b; Qi et al., 2022b and 2023; Zhang et al., 2022). In this study, the Res-UNet architecture was designed with five layers that incorporated the MSI TOA reflectance values at four bands, i.e., B2 (490 nm), B3 (560 nm), B4 (665 nm), and B8a (865 nm), and an alternative floating algae index (AFAI) to measure

the red-edge vegetation reflectance. Prior to being used in the model, each MSI band was normalized to a range of 0–255. AFAI was calculated using MSI B4, B6 (740 nm), and B8a, and then normalized to a range of 0–255 using low and high thresholds of -0.0015 and 0.04, respectively. To facilitate visualization of these small-scale image features in a map, the 10-m resolution features identified by the Res-UNet DL model were aggregated into 10-km grids.

The detection of *S. horneri* features from VIIRS imagery was based on the AFAI method (Qi et al., 2022a). Image pixels containing *S. horneri* show higher AFAI values than those in the surrounding waters. Therefore, after properly masking clouds and other noisy features, *S. horneri* features were extracted using pre-defined threshold values. For visual inspections, the NOAA Ocean Color Viewer (OCView) online tool (Mikelsons and Wang, 2018) also shows these features in the 375 m resolution false-color Red-Green-Blue (FRGB) imagery (e.g., Fig. 1a, also see https://www.star.nesdis.noaa.gov/socd/mecb/color/ocview/ocview.html).

2.3. Numerical experiments

Two numerical experiments were conducted using the same three-dimensional hydrodynamic model but different initialization.

The model was developed for the marginal seas, i.e., the Bohai Sea, YS, ECS, Japan Seas, etc., around China, Korea, Japan, and other countries, based on the Regional Ocean Modeling System (ROMS). The model is a free surface, hydrostatic, primitive equation ocean model that uses stretched, terrain-following vertical coordinates and orthogonal curvilinear horizontal coordinates on an Arakawa-C grid (Haidvogel et al., 2000; Shchepetkin and McWilliams, 2005). With a total of 1001 × 528 grid cells, the orthogonal curvilinear coordinate system was designed to have grid spacing ranging from 1.5 km near the Changjiang River estuary mouth to 11.3 km near the eastern open boundary. The vertical dimension was discretized with 30 sigma layers that have higher resolution near the surface and bottom. The vertical eddy viscosity and diffusivity were computed using the k-ε turbulence closure model. Horizontal eddy viscosity and diffusivity were scaled by grid size, and the coefficient for the largest grid size was set to 1.0 m^2/s.

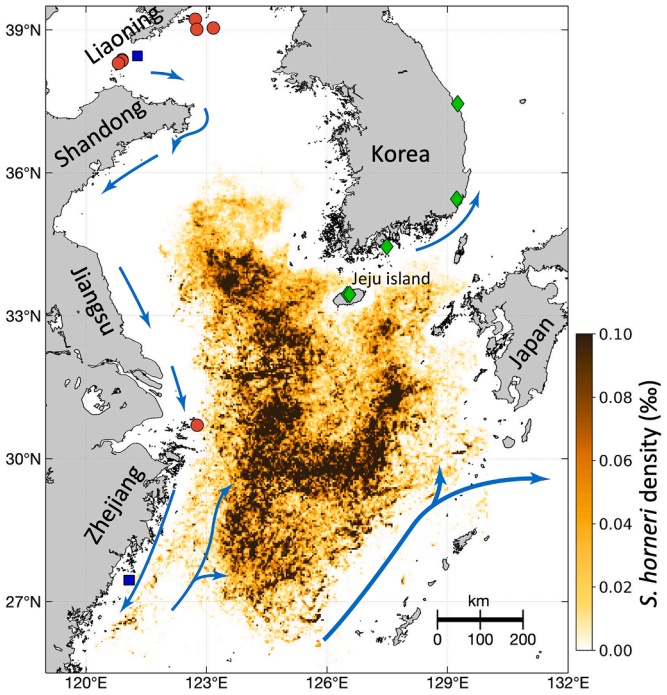

Fig. 2. Cumulative footprint of mean *S. horneri* density in the YS and ECS observed from MODIS during the *S. horneri* peak season of March to May between 2000 and 2021 (adapted from Qi et al., 2022a). The green diamonds, red circles, and blue squares represent locations of benthic samples of *S. horneri* reported in Byeon et al. (2019), Li et al. (2020), and Su et al. (2018), respectively. These symbols serve as indicators of the presence of habitats where floating *S. horneri* in the YS and ECS have originated from. Blue lines indicate the major ocean currents in the fall and winter (Chen 2009).

The model was forced by tides at the offshore open boundary, by river discharge from 10 major rivers along the coast, and by atmospheric forcing on the water surface. Tidal forcing at the open boundary was

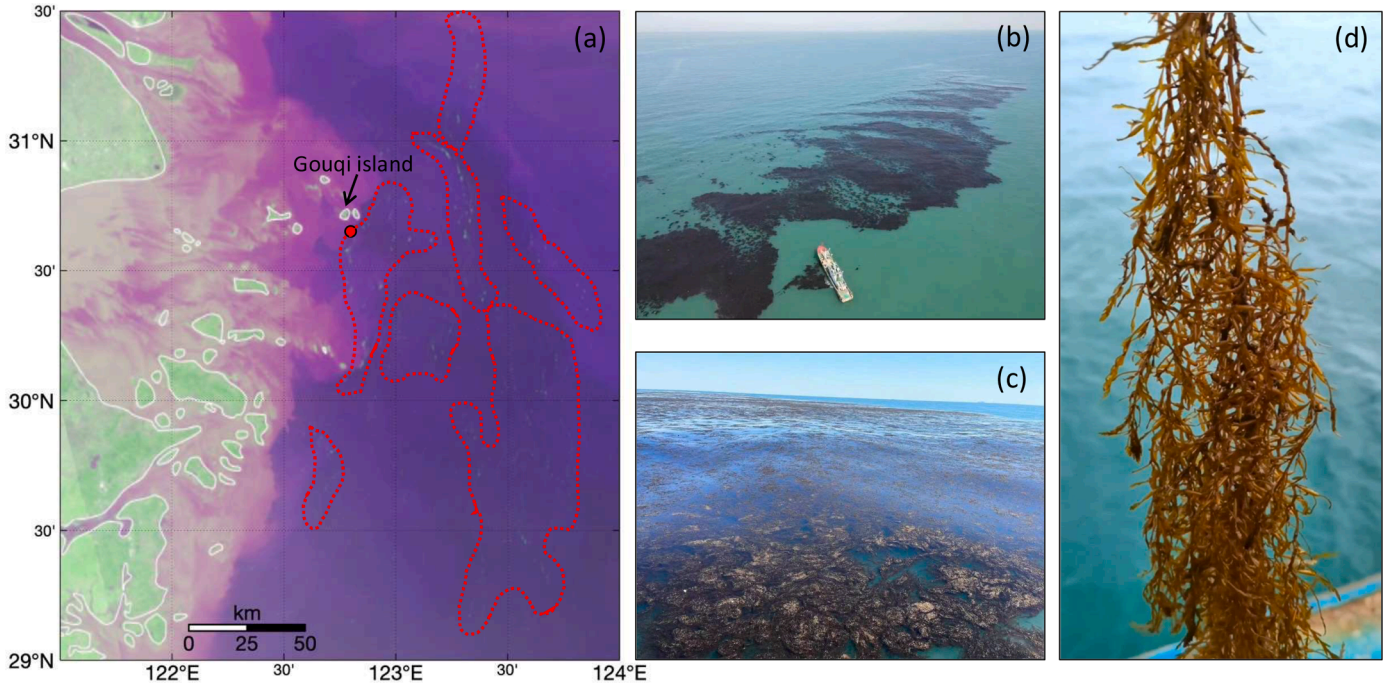

Fig. 1. *S. horneri* in the East China Sea. (a) False-color RGB image on 8 April 2023 from NOAA OCView shows floating *S. horneri* as greenish image slicks, some of which are outlined in red dotted lines. (b)–(d) Photographs of *S. horneri* floating on surface waters taken on the same day near Gouqi Island (red circle in (a)).

specified using the Oregon State University global inverse tidal model TPXO.8.0 (Egbert and Erofeeva, 2002), with all 13 tidal constituents applied. Ambient currents, temperature, and salinity extracted from the global Hybrid Coordinate Ocean Model (HYCOM) (https://www.hycom.org) were nudged into the open boundary with a relaxation timescale of 3 days for inflows. The major rivers included in the model are Han, Yalu, Liaohe, Haihe, Yellow, Changjiang, Qiantang, Mingjiang, Pearl, and Mekong Rivers. Daily river discharge and water temperature data for the Changjiang, Yellow, and Pearl Rivers were available (http://xxfb.hydroinfo.gov.cn), and climatological monthly river discharges for other rivers were obtained from Wu et al. (2021). The atmospheric forcing was extracted from the ERA5 climate reanalysis, which has hourly and 0.25-degree resolutions and is produced by the European Center for Medium-range Weather Forecasts (ECMWF) (https://climate.copernicus.eu/climate-reanalysis). The surface wind stress and net heat fluxes were computed using the bulk parameterization. The numerical implementations were performed from 1 January 2018 to 30 June 2021. The first two years acted as ramp to spin up the model and the hourly modeled velocity fields from 2020 to 2021 were stored. The offline Lagrangian Transport model (LTRANS, North et al., 2008) was applied to track particles with the stored ROMS velocity fields.

In the first experiment, the model was initialized with particles released in the same locations on the same day of the MSI-observed *S. horneri* features. Then, these particles were tracked for 4 months using LTRANS to determine their daily distributions.

In the second experiment, the locations and days to release particles to initialize the model were determined by hypothesized scenarios based on observations and literature review results. This is because, even with high-resolution satellite imagery, the initial occurrence of surface *S. horneri* may be too small to be detected.

3. Results

3.1. Literature review

All publications relevant to the origins of floating *S. horneri* in the ECS are presented in Table 1, together with their methodology and main findings. It is clear that these studies are not entirely consistent on the possible origins of *S. horneri*.

Several studies, such as Filippi et al. (2010), Qi et al. (2017), and Kwon et al. (2019), have utilized in situ observations or medium-resolution satellite imagery, along with numerical models, to trace the origins of the ECS *S. horneri*. The results suggest that the southeastern coast of China or Zhejiang Province may be a potential source of the satellite observed *S. horneri* in the ECS, while the studies also acknowledged that this is likely not the sole source.

Other studies, such as Xing et al. (2017), Chen et al. (2019), Yuan et al. (2022), and Wang et al. (2023), have used high-resolution satellite imagery from GaoFen (GF), MSI and/or Coastal Zone Imager (CZI) to identify small *S. horneri* features before they form into larger features observable in medium-resolution satellite imagery. Small patches of *S. horneri* were observed in the northern YS near Shandong Peninsula during September–October in 2016 and 2020. Yuan et al. (2022) and Wang et al. (2023) suggested that these *S. horneri* patches can travel along two paths: one towards Jiangsu shoal and the other towards Jeju Island, South Korea (Fig. 2). Based on these high-resolution satellite observations, the Shandong Peninsula was thought to be one source region of floating *S. horneri* observed in the YS and ECS.

Recently, the DNA sequencing method has emerged as a valuable tool for tracing the origins of *S. horneri* in the YS and ECS. Several studies, such as Byeon et al. (2019), Su et al. (2018), and Li et al. (2020), have used this method to analyze floating and benthic samples of *S. horneri* from various locations along the coasts of Korea and China (specifically Zhejiang and Liaoning), as marked in Fig. 2. These studies reported two dominating haplotypes. Additionally, Liu et al. (2018b), Zhang et al. (2019), Zhuang et al. (2021), and Zhuang et al. (2022) collected samples from surface waters and aquaculture facilities in the YS and ECS and analyzed their DNA sequence. The results indicate that there are likely two sources of satellite-observed *S. horneri* blooms in the YS and ECS, with Zhejiang being one primary source.

Lastly, Mizuno et al. (2014) and Huang et al. (2018) used in situ surveys, and Zhan et al. (2022) developed the fencing experiment to determine the *S. horneri* origins. In addition to the speculated origins from Zhejiang or Shandong, Huang et al. (2018) suggested that the ECS *S. horneri* in spring 2017 might come from Liaoning, which was supported by the benthic *S. horneri* samples reported by Su et al. (2018) and Li et al. (2020) around Liaoning (Fig. 1).

In summary, despite the numerous studies to determine the possible origins of the floating *S. horneri* in the ECS, the findings are mixed and inconclusive. While some suggested the southeastern coast of China or Zhejiang Province as a potential source, others proposed the Shandong Peninsula or Liaoning Province as another possible origin.

3.2. Multi-year high-resolution image sequence

Reported by Qi et al. (2022a), the peak season of *S. horneri* blooms in

Table 1
Publications relevant to origins of the ECS *S. horneri*, in chronicle order.

Author & year	Observation	Numerical model	DNA	Time of observation	Possible origins
Filippi et al. (2010)	*in situ* (floating samples)	POM*	/	May 2002	China coast of ECS
Mizuno et al. (2014)	*in situ* (floating samples)	/	/		China coast
Qi et al. (2017)	Satellite (MODIS, Landsat)	HYCOM*	/	2012–2017	Zhejiang coast
Xing et al. (2017)	Satellite (GF)	/	/	Oct. 2016–Jan. 2017	Shandong
Huang et al. (2018)	*in situ* survey	/	/	2016–2017	Liaoning
Liu et al. (2018b)	*in situ* (floating samples)	/	Mitochondrial plastid	2016–2017	Two dominating haplotypes
Su et al. (2018)	*in situ* (benthic and floating samples)	/	microsatellite	2012–2016	Multiple sources
Byeon et al. (2019)	*in situ* (benthic and floating samples)	/	Mitochondrial microsatellite	2015–2018	Possibly Zhejiang, two clusters
Chen et al. (2019)	Satellite (GF, Landsat)	/	/	Oct. 2016–Jan. 2017	Shandong
Kwon et al. (2019)	Satellite (GOCI)	ROMS*, LTRANS*	/	May 2017	Southeastern coast of China
Zhang et al. (2019)	Satellite (HJ); in situ (floating samples)	/	Mitochondrial ribosomal	Apr.–Nov. 2017	Zhejiang
Chen et al. (2019)	Satellite (GF, Landsat)	/	/	Oct. 2016–Jan. 2017	Shandong
Li et al. (2020)	*in situ* (benthic and floating samples)	/	Mitochondrial	2015–2019	Two dominating haplotypes
Zhuang et al. (2021)	*in situ* (floating samples)	/	Mitochondrial	2017–2019	ECS
Yuan et al. (2022)	Satellite (MSI, GF, CZI)	/	/	Sep. 2019–Jul. 2020	A non-Zhejiang source
Zhan et al. (2022)	*in situ* (Fencing experiment)	/	/	Nov. 2018–Oct. 2019	China coast of YS and ECS
Zhuang et al. (2022)	*in situ* (benthic and floating samples)	/	Mitochondrial	2017–2021	Shandong
Wang et al. (2023)	Satellite (MSI, GF, CZI)	/	Mitochondrial plastid	2017–2021	Another source in ECS

POM: Princeton Ocean Model (Mellor, 2003); HYCOM: The Hybrid Coordinate Ocean Model (Bleck and Boudra, 1981); ROMS: Regional Ocean Modeling System (Shchepetkin and McWilliams, 2005); LTRANS: The Larval TRANSport Lagrangian model (North et al., 2008).

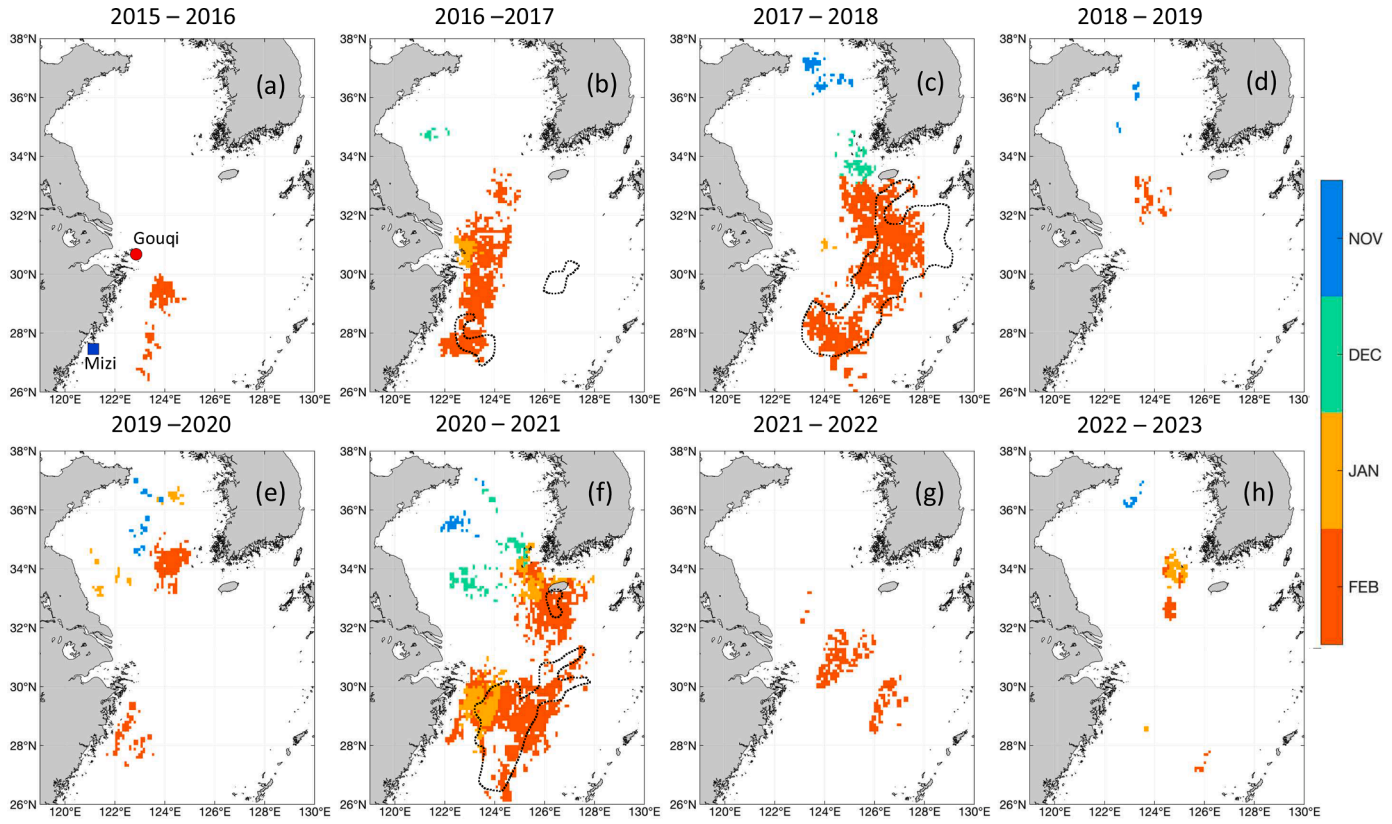

Fig. 3. (a)–(h): *S. horneri* features captured in high-resolution MSI imagery during the months of November, December, January, and February in 2015–2023. The original image features had a resolution of 10-m per pixel but were aggregated into 10-km grids to help visualization. Black dashed lines in panels (b), (c), and (f) outline the locations of *S. horneri* that are also visible in VIIRS imagery (375-m resolution) in February. No *S. horneri* features could be observed in either VIIRS or MODIS imagery before February. The locations of Gouqi Island and Mizi Island are marked in (a) as a red circle and a blue square, respectively.

the ECS is typically between April and May, and a large quantity of *S. horneri* in the YS can sometimes be observed in March. The large *S. horneri* image features can also be visible from the medium-resolution VIIRS or MODIS images as early as February, as indicated by the black outlines in Fig. 3b, c, and f. However, several studies (Chen et al., 2019; Wang et al., 2023; Xing et al., 2017; Yuan et al., 2022) have reported *S. horneri* image features from high-resolution images even before February in certain years, suggesting that the initial occurrence of *S. horneri* can only be detected in high-resolution images.

Fig. 3 shows the temporal evolution of *S. horneri* features detected from the 10-m resolution MSI images during the late fall and winter seasons (November–February) in the YS and ECS from November 2015 to February 2023, with each month color coded to facilitate visualization. The locations of floating *S. horneri* determined from the VIIRS images in February are outlined in black. Due to the medium resolution (375 m), VIIRS did not show any *S. horneri* image features prior to February, and in most years such detections were not possible even in February.

3.2.1. *S. horneri around the Shandong Peninsula*

Earlier studies using high-resolution satellite imagery revealed *S. horneri* movement from waters around the Shandong Peninsula in October 2016 to waters near Jiangsu Shoal in January 2017 (Xing et al., 2017; Chen et al., 2019). Yuan et al. (2022) further showed two different drifting pathways from Shandong to Jiangsu Shoal and Jeju Island (Korea), respectively, from October 2019 to April 2020. The MSI image sequences in Fig. 3b and e show consistent patterns as with those from earlier studies although some of the *S. horneri* features were missed due to the relatively narrow swath of MSI (290 km).

In addition to the two years of 2016–2017 and 2019–2020, the MSI image sequences revealed similar drifting pathways in other years as well, with the earliest satellite-detectable *S. horneri* features in November around the northeastern tip of the Shandong Peninsula (Fig. 3c, d, f, and h). Between November 2020 and February 2021, large amounts of *S horneri* started to appear in the northern YS in November 2020, with a major bloom found in February 2021 near Jeju Island (Fig. 3f). However, the first appearance of *S. horneri* in satellite imagery in October–November near the Shandong Peninsula does not necessarily indicate the origin from the same locations because 1) the initial floating *S. horneri* could be too small to be detected even in high-resolution satellite imagery; 2) there is no report of benthic *S. horneri* around the Shandong Peninsula; and 3) the possibility of other origins with different timings still exists.

3.2.2. *S. horneri near the Zhejiang coast*

In addition to the October–November appearance of *S. horneri* features in MSI imagery around the Shandong Peninsula, *S. horneri* can often be observed in January or February near the Zhejiang coast, and these features appear to be disconnected from those around the Shandong Peninsula, possibly indicating a separate origin. The yellow colors in Fig. 3b, c, f, and h all show *S. horneri* features in January, which moved towards the east as driven by the Changjiang Diluted Water (CDW) current. During this time, *S. horneri* tended to proliferate rapidly in the following month of February, owing to a rise in sea surface temperature (SST) to around 14 °C, which is highly conducive to *S. horneri* growth (Yu et al., 2019).

Based on satellite observations and numerical modeling, several studies suggested that the Zhejiang coast could be an important source of *S. horneri* blooms in the ECS (Filippi et al., 2010; Qi et al., 2017). Furthermore, numerous studies reported that Gouqi island (Fig. 3a, marked as a red circle) is rich in benthic *S. horneri*, and this is also where the *S. horneri* features first appeared in MSI imagery in January. In

contrast, although Mizi island (Fig. 3a, marked as a blue square) on the southern coast of Zhejiang was also reported to be rich in benthic *S. horneri, S. horneri* features were captured in MSI imagery around this island before February. Overall, these satellite-based observations suggest that the area around Gouqi island could be a potential source of floating *S. horneri* in the ECS.

3.2.3. *S. horneri near Liaoning coast*

Huang et al. (2018) conducted an in situ survey, which suggested that coastal waters off Liaoning coast could potentially be a source of the observed floating *S. horneri* in the Yellow Sea. This finding was further supported by the benthic samples of *S. horneri* in the area shown in Fig. 2 (Li et al., 2020; Su et al., 2018). Additionally, local news reports have indicated the presence of floating *S. horneri* near Dalian in Liaoning Province in recent years (Runsky, 2020).

Here, MSI images over the Bohai Sea showed *S. horneri* features in October and November 2020 near Dalian in Liaoning Province (Fig. 4a). These image features were determined to be due to *S. horneri* because they showed typical characteristics of *S. horneri* reflectance (Fig. 4b and c). Specifically, both the reflectance spectra from selected pixels of the MSI image features and the reflectance spectra collected from in situ measurements over *S. horneri* mats show the typical red-edge reflectance (i.e., enhanced reflectance in the near-infrared bands of > 700 nm) and low reflectance in all visible bands, confirming the presence of *S. horneri* in the former case. The sequential MSI images also indicated the southward or southeastward drifting pathways of *S. horneri* from October to November 2020. These observations reinforce the possibility that coastal waters off Liaoning Province could be a source region of *S. horneri* observed in the YS in latter months.

To summarize, multi-year MSI imagery revealed the presence of weak *S. horneri* features in the vicinity of Shandong, Zhejiang, and Liaoning Provinces prior to the formation of large *S. horneri* blooms captured in medium-resolution satellite imagery in the YS and ECS as reported in earlier studies. The in situ surveys and benthic samples further supported the hypothesis that these *S. horneri* blooms could have originated from Zhejiang and Liaoning coastal waters. However, the drifting pathways of the MSI-observed *S. horneri* still require further investigation using numerical experiments, as shown below. Likewise, due to coverage gaps caused by clouds and other factors, remote sensing imagery may not provide a complete sequence of the initial appearance and temporal changes of *S. horneri*, which numerical experiments may overcome.

3.3. *Numerical experimental results*

3.3.1. *Model initialized by MSI observations*

Fig. 5a–c show the modeled particle trajectories and distributions when the ROMS model was initialized using the MSI-detected *S. horneri* locations on 18 October, 11 November, and 21 December 2020, respectively. These particles were tracked until 6 April 2021, when large amounts of *S. horneri* were detected in the medium-resolution VIIRS imagery. In these figures, the solid black outlines illustrate the locations where *S. horneri* features were captured in MSI images, where and when particles were released in the model. The color-coded points denote the particle locations at different times, with warm colors indicating later dates and red color indicating 6 April 2021. For reference, *S. horneri* features observed from the VIIRS image on the last day of the model simulation (6 April 2021) are overlaid as black symbols.

In Fig. 5a, the model was initialized by particles near Liaoning on 18 October 2020 (Group A in Fig. 5a). These particles were advected by ocean currents into the YS, passing around the northeastern tip of the Shandong Peninsula. It took 2–5 months for the particles to reach the Shandong Peninsula. Therefore, the *S. horneri* features observed on November 11 in the MSI image to the east of the Shandong Peninsula (i.e., Group B in Fig. 5b) could not be a result of Group A released in mid-October but could be a result of *S. horneri* in the same location of Group A at an earlier time, as shown in the hypothesized initiation below.

The *S. horneri* features observed in the MSI image on 11 November 11 2020, east of the Shandong Peninsula (Group B in Fig. 5b), drifted further to the south and southeast, driven by ocean currents, reaching

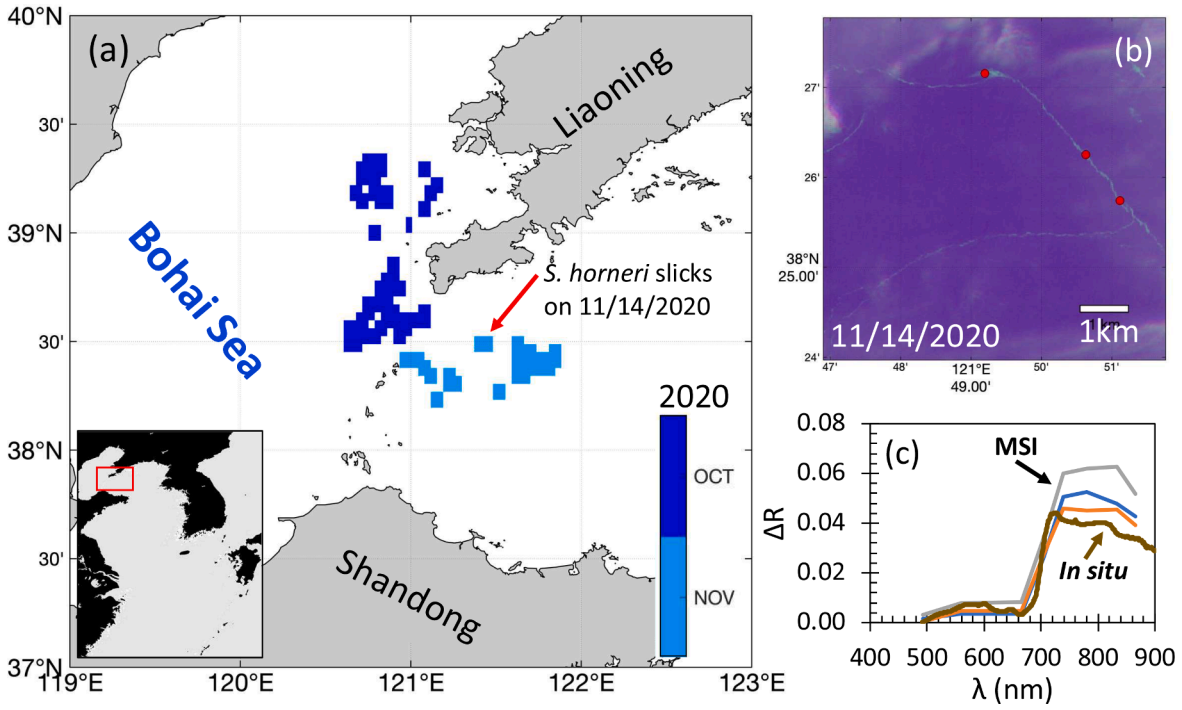

Fig. 4. (a) *S. horneri* features observed in MSI imagery in the Bohai Sea (location shown in the inset map) near Liaoning coast during autumn of 2020. The original image features had a resolution of 10-m per pixel but were aggregated into 10-km grids to help visualization. (b) MSI image features observed on 14 November 2020, corresponding to the location pointed by the red arrow in (a). The red circles indicate the locations where MSI spectra were extracted and shown in panel (c). The brown line in (c) represents the in situ spectra of floating *S. horneri* obtained from the ECS in April 2021.

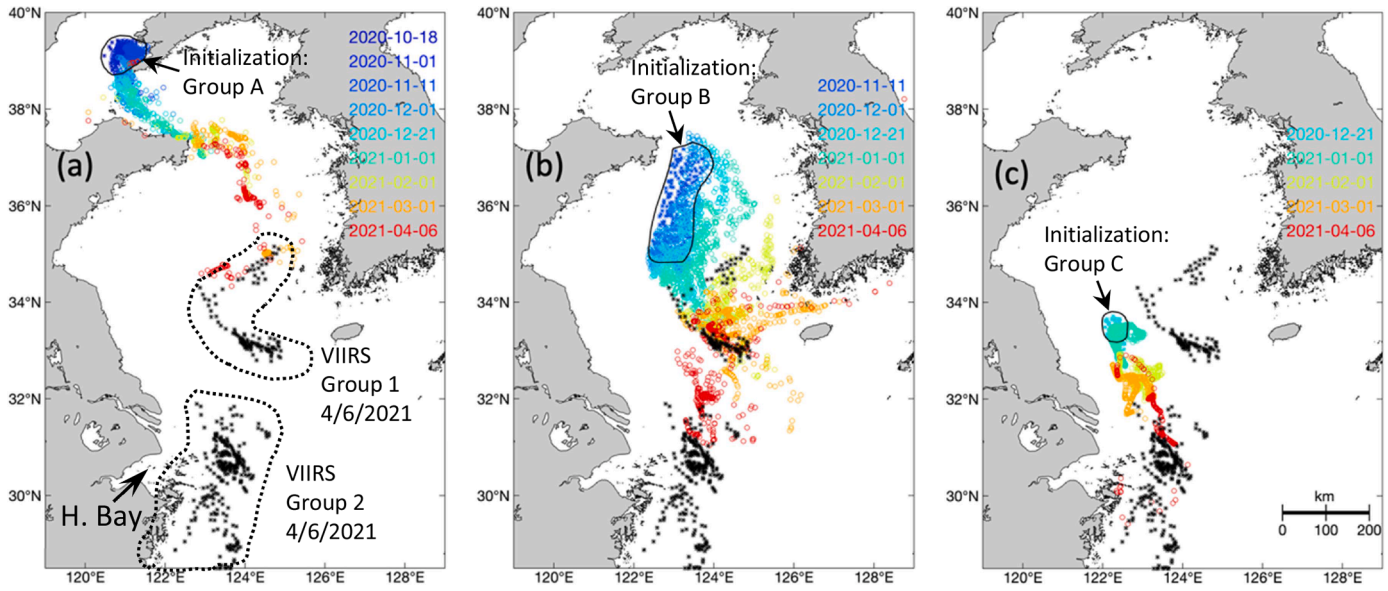

Fig. 5. Results of the first numerical experiment where the ROMS model was initialized with particles released at the MSI-observed locations and times (solid black outlines), and then followed until 6 April 2021 for (a)–(c) model initialization on October 18, November 11, and December 21, respectively. Black symbols represent *S. horneri* features observed in the VIIRS image on 6 April 2021. Note that most satellite-observed *S. horneri* south of Hangzhou Bay (dotted outline, where Hangzhou Bay is annotated with an arrow in (a)) cannot be explained by the model simulations, thus indicating different origins than the model initialization locations.

the southern YS up to the Yangtze River mouth by early April (Fig. 5b). The *S. horneri* features observed in the VIIRS image on 6 April 2021, to the north of the Yangtze River mouth (labeled as VIIRS Group 1 in Fig. 5a), are likely a result of this drift. In contrast, most of the VIIRS-observed *S. horneri* on the same day but to the south of the Yangtze River mouth (labeled as VIIRS Group 2 in Fig. 5a) cannot be explained by this same drift, thus indicating another possible origin.

In addition to the two model initializations of Fig. 5a and b, Fig. 5c shows the simulation results from the third initialization in Group C, based on *S. horneri* observations in the MSI image on 21 December 2020. According to the simulation results in Fig. 5a and b, Group C is not within the drifting pathways in those two scenarios, therefore could be a result of the same speculated source region near the Liaoning coast but with floating *S. horneri* occurring earlier than October. The model simulations showed that particles in Group C moved southward to reach the vicinity of the Yangtze River mouth by early April. Only a very small portion of the particles can drift across the Yangtze River plume and continue to move southward, suggesting that the majority of the *S. horneri* in the VIIRS Group 2 (Fig. 5a) may have a different origin than that from the north.

3.3.2. *Model initialized by hypothesized S. horneri locations and timings*

The numerical experiments above suggest that the VIIRS-observed *S. horneri* to the north of the Yangtze River mouth (VIIRS Group 1 in Fig. 5a) on 6 April 2021 could have been a result of *S. horneri* drifting from the north, but such drifting could not explain the *S. horneri* features observed in the same VIIRS image but to the east and south of the Yangtze River mouth (VIIRS Group 2 in Fig. 5a). There must be another source to support this latter observation, and such a source could be around Gouqi Island because benthic *S. horneri* has been reported around the island. Indeed, *S. horneri* image features have been observed in this area every January or February since 2016.

Furthermore, as shown in Figs. 3f and 5a–c, S. *horneri* in the YS between November and December 2020 could have originated from the Liaoning coast where the initial floating *S. horneri* would take 2–5 months to reach the YS. The non-explained Group C in Fig. 5c suggests that the initial appearance of floating *S. horneri* around the Liaoning coast may be earlier than October. Indeed, local news in Dalian (Liaoning Province) reported relatively large amounts of floating *S. horneri* in the vicinity of the Dalian coast during early summer (Runsky, 2020).

Based on these observations and analysis, we hypothesize the following two origins and timings of initial floating *S. horneri* that led to large blooms in the YS and ECS: the first being an area around the Dalian coast in June and the second being a region around Gouqi Island in January.

To test this hypothesis, the ROMS model was initiated by particles in the two possible origins in their respective time frame: Dalian coast on 1 June 2020 and Gouqi Island on 1 January 2021, with results presented in Fig. 6a and b, respectively.

Fig. 6a shows that if the initial floating *S. horneri* appeared in June 2020 around Dalian, the satellite-observed *S. horneri* patterns (e.g., the black symbols to the north of the Yangtze River mouth or VIIRS Group 1 in Fig. 5a, and those from MSI observations in Fig. 5b and c) in the later months could be well explained by the current-driven particle drifting. Likewise, Fig. 6b shows that if the initial floating *S. horneri* appeared in January 2021 around Gouqi Island, the VIIRS-observed *S. horneri* to the east and south of the Yangtze River mouth (i.e., VIIRS Group 2 in Fig. 5a) could also be explained by the current-driven particle drifting. Note that these patterns could not be explained by *S. horneri* that drifted from the north with the same Dalian origin (Fig. 5).

3.3.3. *Conceptual illustration*

Based on these observations, a conceptual illustration is presented in Fig. 7 to summarize the two possible origins, their respective timings of first occurrence of floating *S. horneri*, as well as their general drifting pathways. Specifically, benthic *S. horneri* around the Dalian coast (origin # 1 in Fig. 7a) may be detached in June, and then be transported by ocean currents to reach the YS and north ECS by March or early April, during which *S. horneri* can grow into relatively large mats. Benthic *S. horneri* around Gouqi Island (origin # 2 in Fig. 7d), on the other hand, may be detached in January, and then be transported by ocean currents to the south and east to form large mats by March or early April. *S. horneri* is then transported further to the east and northeast to reach Jeju Island (Korea, Fig. 7a, marked as a red triangle), and further transported northwest to the north ECS and YS by May. During all transports, *S. horneri* on the ocean surface continues to grow because of the favorable temperature, nutrient availability, and ambient light,

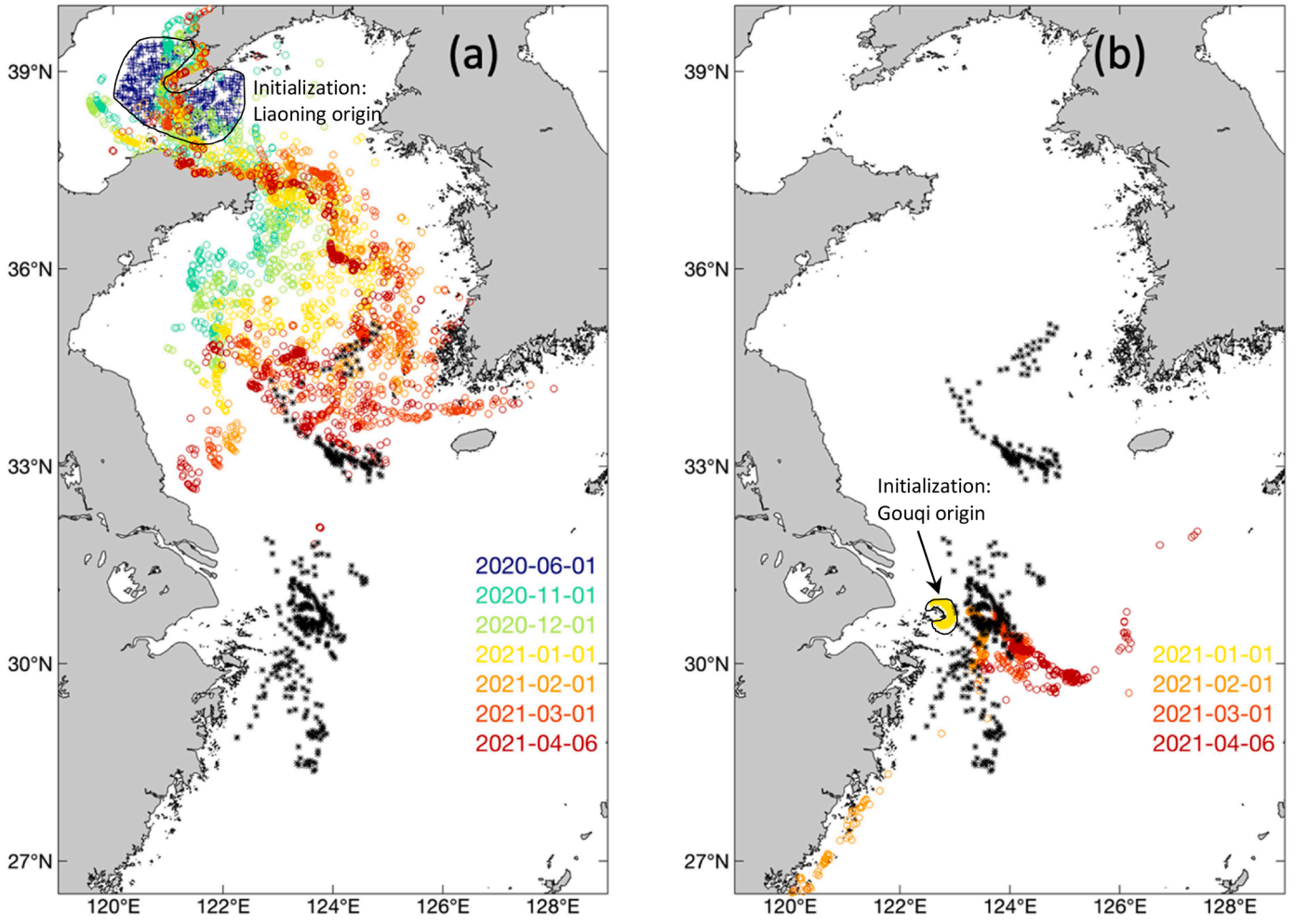

Fig. 6. Similar to Fig. 5, but the ROMS model was initialized by particles released in hypothesized locations and times on 1 June 2020 in the Bohai Sea (a) and 1 January 2021 off Hangzhou Bay (b), respectively (solid outlines), and followed until 6 April 2021. Similar to Fig. 5, the black symbols represent *S. horneri* features observed in the VIIRS image on 6 April 2021. In contrast to Fig. 5, VIIRS observed *S. horneri* patterns could be reproduced by the model simulations (colored dots) in (b).

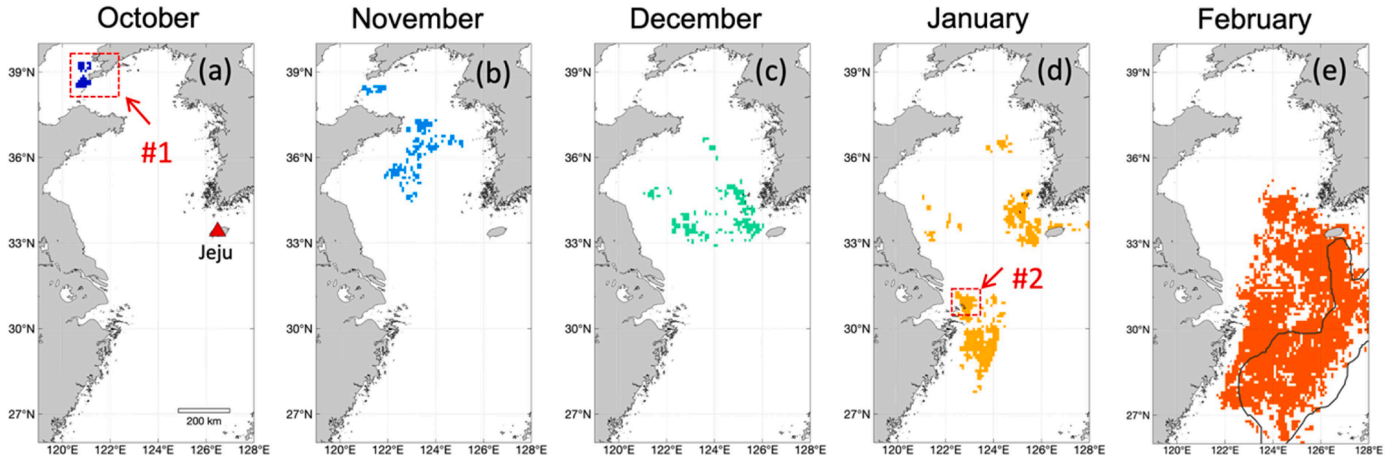

Fig. 7. (a)–(e) Climatological monthly distributions of floating *S. horneri* observed from MSI between 2015 and 2023 show two possible origins of *S. horneri* (dashed rectangles annotated as #1 and #2 in (a) and (d), respectively), with their approximate timings and transport pathways. The location of Jeju Island (Korea) is annotated as a triangle in (a). The black line in (e) shows the MODIS climatology observation of *S. horneri* from 2000 to 2021 (Qi et al., 2022). *S. horneri* cannot be detected by MODIS from October to January due to its low density during those months.

resulting in maximum *S. horneri* amounts in April or May (Qi et al., 2022a). After May, because the water temperature is too high for *S. horneri* (Choi et al., 2007; Yu et al., 2019; Qi et al., 2022a; Shin et al., 2022) and/or because of an innate biological clock (circannual rhythm) as observed in other brown seaweeds (Lüning, 1994), S. *horneri* gradually dies and sinks to the ocean floor, resulting in minimal satellite-observed amounts (Qi et al., 2022a).

4. Discussion

4.1. Strengths and weaknesses of high-resolution remote sensing and numerical experiments

The current study is certainly not the first to combine remote sensing and numerical models to understand the drifting pathways or possible origins of *S. horneri* (e.g., Filippi et al., 2010; Kwon et al., 2019; Qi et al., 2017; Table 1). However, this is the first to have multi-year high--resolution observations together with both observation-based model initialization and hypothesis-based model initialization, which led to the findings of two possible origins with different timings of initial floating *S. horneri* that could explain satellite-observed *S. horneri* when large amounts were detected in the ECS and YS. In particular, high-resolution remote sensing imagery provided information on the location and timing of floating *S. horneri* that would be difficult to detect from medium-resolution imagery. In addition, the regional ROMS model proved to be a valuable tool to track surface features to fill data gaps in remote sensing imagery due to clouds or lack of orbital coverage.

However, neither remote sensing nor numerical modeling could provide complete information to reproduce observations of large amounts of *S. horneri* in the ECS and YS. For example, although the earliest images showing *S. hornei* features were used to initialize the model, the actual occurrence date could be earlier and the occurrence location could be different, both due to clouds and lack of orbital coverage. This is also why hypothesized locations and timings were used to initialize the model. On the other hand, the model is purely based on physical transport without considering any biological processes (i.e., growth or mortality of *S. horneri*). This is why the model results were interpreted qualitatively to compare the large-scale patterns with satellite observations. However, the general agreement in locations between the simulated and satellite-observed *S. horneri* by early April suggests the usefulness of the ROMS model in inferring the possible origins of the ECS floating *S. horneri*. In particular, the numerical experimental results clearly showed that *S. horneri* from the north could not be transported to the south of the Yangtze River mouth, possibly due to the Yangtze River ring front (Liu et al., 2018a) that may serve as a "wall" to prevent particle drifting. Such a "wall" effect has been observed for surface oil slicks in the Gulf of Mexico (Androulidakis et al., 2018; Kuitenbrouwer et al., 2018) and surface scums of *Noctiluca scintillas* in the ECS (Qi et al., 2022c). This also suggests that *S. horneri* to the south of the Yangtze River ring front in January–February likely originated from the Zhejiang coast (Gouqi Island), which further developed into large blooms in the ECS in April–May.

Another limitation of this study is its lack of ability to track the floating *S. horneri* back to any possible benthic populations from natural seaweed beds or those attached on the surface aquaculture rafts along the coasts. With the very similar geographic distribution of both types of populations, it is almost impossible to tell the difference between them and assess their contributions to the observed golden tides solely by the high-resolution remote sensing imagery or numerical tracking. This challenge is also faced by other techniques. For example, even the molecular technique (DNA sequencing) could not tell whether the YS-ECS *S. horneri* is from benthic or surface populations in the proposed origins (Byeon et al., 2019; Su et al., 2018; Li et al., 2020). Although the genetic makeup of benthic *S. horneri* samples collected from the Shandong coast is more like the *S. horneri* samples in the YS than to those from the Zhejiang or Liaoning coasts (Zhuang, 2022), it is doubtful that these *S. horneri* samples are transported from the Shandong coast to the satellite-observed *S. horneri* in the YS. This is because the dominant regional ocean currents in winter are in the northeast–southwest direction along the Shandong coast (Chen, 2009) as opposed to the northwest-southeast direction to the YS. On the other hand, regardless of the difficulty in differentiating benthic and surface-floating *S. horneri*, the ability to track the geographic origins by the high-resolution satellite imagery and numerical experiments provides essential information to help design in situ experiments in the two proposed origins to address this challenge.

4.2. Different timings in the two origins

The high-resolution remote sensing observations and numerical experiments suggest not only two remote origins of floating *S. horneri* in the ECS, both in the intertidal zones rich in benthic *S. horneri*, but also different timings of their first occurrence as floating *S. horneri* (Fig. 7). Although the exact reason behind the different timings is not clear, there are possibly two factors. The first may be related to their respective types. According to the summary by Huang et al. (2018), *S. horneri* in Liaoning and Zhejiang coastal regions belongs to the summer-maturing type and the spring-maturing type, respectively. The second may be related to temperature. Although the timing is different, the water temperature is about the same in both regions during their respective timings, i.e., ~10°C around Dailian in June and Gouqi Island in January.

The first appearance of floating *S. horneri* around Gouqi Island in January suggests that the benthic *S. horneri* is detached from the bottom rocks before the maturation period of April–May during which *S. horneri* releases gametes (Sun and Zhuang, 2009). This also explains why the floating *S. horneri* originating in this area continues to grow at the sea surface until the peak months of April–May. In contrast, there is limited field research on the growth cycle *of S. horneri* near the Liaoning coast, but the local news reports, as well as the analysis here, suggest that the benthic *S. horneri* can be detached from the bottom rocks in June and continue to grow until at least February during the southward drifting. In any case, it is essential to conduct further investigations on *S. horneri* growth cycles in these two source regions to understand why *S. horneri* is detached from the bottom at specific times and to understand the mechanisms leading to *S. horneri* blooms in the ECS. Likewise, because *S. horneri* from coastal aquaculture rafts may also contribute to the observed *S. horneri* image features, it is also important to design in situ experiments to determine whether *S. horneri* on the rafts serves as a source of the offshore *S. horneri* or represents a consequence from offshore drifting *S. horneri*.

5. Summary and conclusion

Through literature review, multi-year high-resolution satellite observations, and carefully designed numerical experiments, we attempted to solve the puzzle of where the recurrent *S. horneri* blooms in the ECS originated, with the following findings:

1 Two possible origins, about 800 km apart, have been identified: one in coastal waters off Dalian of Liaoning Province, and the other in coastal waters around Gouqi Island of Zhejiang Province.
2 The initial occurrence of surface floating *S. horneri* in these two origins is likely to be June and January, respectively, which drift to the YS and ECS following the dominant ocean currents.
3 *S. horneri* mats from the first origin can hardly drift to the south of the Yangtze River mouth, possibly due to the Yangtze River ring front formed by the strong currents, including the Changjiang Dilute Water (CDW).
4 Because of this physical "barrier," most of the floating *S. horneri* in the ECS is likely to be a result of Gouqi origin and continuous growth during the surface drifting.

The study shows the value of combining high-resolution satellite observations and a numerical model in tracking and inferring the possible origins of large-scale *S. horneri* blooms. Yet such inference still requires more observations (particularly time-series observations in the field) to validate and better understand the growth cycles of *S. horneri*, as well as to understand how they respond to environmental changes in the different locations.

Declaration of Competing Interest

The authors declare that they have no known competing financial interests or personal relationships that could have appeared to influence the work reported in this paper.

Data availability

Data will be made available on request.

Acknowledgments

This research was supported by the National Natural Science Foundation of China (Nos. 42076008; 42076180), and the Joint Polar Satellite System (JPSS) funding performed under the contract ST13301CQ0050/1332KP22FNEED004. We thank Dr. Xiumei Zhang from Zhengjiang Ocean University and Dr. Chengfeng Le from Zhejiang University for providing digital photos of *Sargassum horneri* in the East China Sea in April 2023. We also thank two anonymous reviewers for their valuable suggestions to improve the presentation of this work. The scientific results and conclusions, as well as any views or opinions expressed herein, are those of the author(s) and do not necessarily reflect those of NOAA or the Department of Commerce.

References

Androulidakis, Y., Kourafalou, V., Ozgokmen, T., Garcia-Pineda, O., Lund, B., Le Henaff, M., Hu, C., Haus, B.K., et al., 2018. Influence of river-induced fronts on hydrocarbon transport: a multiplatform observational study. J. Geophys. Res. Oceans 123. https://doi.org/10.1029/2017JC013514.

Bleck, R., Boudra, D.B., 1981. Initial testing of a numerical ocean circulation model using a hybrid (Quasi-Isopycnic) vertical coordinate. J. Phys. Oceanogr. 11 (6), 755–770. https://doi.org/10.1175/1520-0485(1981)011<0755:ITOANO>2.0.CO;2.

Byeon, S.Y., Oh, H.J., Kim, S., Yun, S.H., Kang, J.H., Park, S.R., Lee, H.J., 2019. The origin and population genetic structure of the 'golden tide' seaweeds, *Sargassum horneri*, in Korean waters. Sci. Rep. 9 (1), 7757. https://doi.org/10.1038/s41598-019-44170-x.

Chen, C.T.A., 2009. Chemical and physical fronts in the Bohai, Yellow and East China Seas. J. Mar. Syst. 78 (3), 394–410. https://doi.org/10.1016/j.jmarsys.2008.11.016.

Chen, Y., Wan, J., Zhang, J., Ma, Y., Wang, L., Zhao, J., Wang, Z., 2019. Spatial-temporal distribution of golden tide based on high-resolution satellite remote sensing in the South Yellow Sea. J. Coastal Res. 90 (SI), 221–227. https://doi.org/10.2112/si90-027.1.

Choi, H.G., Lee, K.H., Yoo, H.I., Kang, P.J., Kim, Y.S., Nam, K.W., 2007. Physiological differences in the growth of *Sargassum horneri* between the germling and adult stages. J. Appl. Phycol. 20 (5), 729. https://doi.org/10.1007/s10811-007-9281-5.

Runsky. (2020, June 1). *Sargassum horneri* "besieging" Xinghai Bay in Dalian! over 10 tons cleared daily. Dalian Runsky. Retrieved from https://dalian.runsky.com/2020-06/01/content_6049710.html.

Egbert, G.D., Erofeeva, S.Y., 2002. Efficient inverse modeling of barotropic ocean tides. J. Atmos. Oceanic Technol. 19 (2), 183–204. https://doi.org/10.1175/1520-0426(2002)019<0183:EIMOBO>2.0.CO;2.

Filippi, J.B., Komatsu, T., Tanaka, K., 2010. Simulation of drifting seaweeds in East China Sea. Ecol. Inform. 5 (1), 67–72. https://doi.org/10.1016/j.ecoinf.2009.08.011.

Haidvogel, D.B., Arango, H.G., Hedstrom, K., Beckmann, A., Malanotte-Rizzoli, P., Shchepetkin, A.F., 2000. Model evaluation experiments in the North Atlantic Basin: simulations in nonlinear terrain-following coordinates. Dyn. Atmos. Oceans 32 (3), 239–281. https://doi.org/10.1016/S0377-0265(00)00049-X.

Hu, C., Qi, L., Hu, L., Cui, T., Xing, Q., He, M., Wang, N., Xiao, Y., Sun, D., Lu, Y., Yuan, C., Wu, M., Wang, C., Chen, Y., Xu, H., Sun, L.E., Guo, M., Wang, M., 2023a. Mapping *Ulva prolifera* green tides from space: a revisit on algorithm design and data products. Int. J. Appl. Earth Obs. Geoinf. 116, 103173 https://doi.org/10.1016/j.jag.2022.103173.

Hu, C., Zhang, S., Barnes, B.B., Xie, Y., Wang, M., Cannizzaro, J.P., English, D.C., 2023b. Mapping and quantifying pelagic Sargassum in the Atlantic Ocean using multi-band medium-resolution satellite data and deep learning. Remote Sens. Environ. 289, 113515 https://doi.org/10.1016/j.rse.2023.113515.

Huang, B., Ding, L., Qin, S., Fu, W., Lu, Q., Liu, Z., Pang, Y., Li, X., Sun, Z., 2018. the taxonomical status and biogeographical distribution of *sargassum horneri* with the origin analysis of its drifting population in the end of 2016 at the western Yellow Sea. Oceanol. Limnol. Sin. 01, 214–223.

Komatsu, T., Mizuno, S., Natheer, A., Kantachumpoo, A., Tanaka, K., Morimoto, A., Hsiao, S.T., Rothäusler, E.A., Shishidou, H., Aoki, M., 2014. Unusual distribution of floating seaweeds in the East China Sea in the early spring of 2012. J. Appl. Phycol. 26 (2), 1169–1179. https://doi.org/10.1007/s10811-013-0152-y.

Komatsu, T., Tatsukawa, K., Filippi, J.B., Sagawa, T., Matsunaga, D., Mikami, A., Ishida, K., Ajisaka, T., Tanaka, K., Aoki, M., 2007. Distribution of drifting seaweeds in eastern East China Sea. J. Mar. Syst. 67 (3), 245–252. https://doi.org/10.1016/j.jmarsys.2006.05.018.

Kuitenbrouwer, D., Reniers, A., MacMahan, J., et al., 2018. Coastal protection by a small scale river plume against oil spills in the Northern Gulf of Mexico. Cont. Shelf. Res. 163, 1–11.

Kwon, K., Choi, B.J., Kim, K.Y., Kim, K., 2019. Tracing the trajectory of pelagic Sargassum using satellite monitoring and Lagrangian transport simulations in the East China Sea and Yellow Sea. Algae 34 (4), 315–326. https://doi.org/10.4490/algae.2019.34.12.11.

Li, J.J., Liu, Z.Y., Zhong, Z.H., Zhuang, L.C., Bi, Y.X., Qin, S., 2020. Limited genetic connectivity among sargassum horneri (Phaeophyceae) populations in the Chinese Marginal Seas despite their high dispersal capacity. J. Phycol. 56 (4), 994–1005. https://doi.org/10.1111/jpy.12990.

Liu, D., Wang, Y., Wang, Y., Keesing, J.K., 2018a. Ocean fronts construct spatial zonation in microfossil assemblages. Global Ecol. Biogeogr. 27 (10), 1225–1237. https://doi.org/10.1111/geb.12779.

Liu, F., Liu, X., Wang, Y., Jin, Z., Moejes, F.W., Sun, S., 2018b. Insights on the *Sargassum horneri* golden tides in the Yellow Sea inferred from morphological and molecular data. Limnol. Oceanogr. 63 (4), 1762–1773. https://doi.org/10.1002/lno.10806.

Lüning, K., 1994. When do algae grow? the third founders' lecture. Eur. J. Phycol. 29 (2), 61–67.

Mellor, G., 2003. Users guide for a three-dimensional, primitive equation, numerical ocean model. Prog. Atmos Ocean. Sci. 4–21.

Mikelsons, M., Wang, M., 2018. Interactive online maps make satellite ocean data accessible, 99. Eos, Washington DC. 10.1029/2018EO096563.

Mizuno, S., Ajisaka, T., Lahbib, S., Kokubu, Y., Alabsi, M., Komatsu, T., 2014. Spatial distributions of floating seaweeds in the East China Sea from late winter to early spring. J. Appl. Phycol. 26 (2), 1159–1167. https://doi.org/10.1007/s10811-013-0139-8.

North, E., Schlag, Z., Hood, R., Li, M., Zhong, L., Gross, T., Kennedy, V., 2008. Vertical swimming behavior influences the dispersal of simulated oyster larvae in a coupled particle-tracking and hydrodynamic model of Chesapeake Bay. Mar. Ecol. Prog. Ser. 359, 99–115.

Qi, L., Hu, C., Barnes, B.B., Lapointe, B.E., Chen, Y., Xie, Y., Wang, M., 2022a. Climate and anthropogenic controls of seaweed expansions in the East China Sea and Yellow Sea. Geophys. Res. Lett. 49 (19) https://doi.org/10.1029/2022GL098185 e2022GL098185.

Qi, L., Hu, C., Liu, J., Ma, R., Zhang, Y., Zhang, S., 2022c. Noctiluca blooms in the East China Sea bounded by ocean fronts. Harmful Algae 112, 102172. https://doi.org/10.1016/j.hal.2022.102172.

Qi, L., Hu, C., Wang, M., Shang, S., Wilson, C., 2017. Floating algae blooms in the East China Sea. Geophys. Res. Lett. 44 (22), 501–511. https://doi.org/10.1002/2017GL075525, 11509.

Qi, L., Wang, M., Hu, C., Holt, B., 2022b. On the capacity of Sentinel-1 synthetic aperture radar in detecting floating macroalgae and other floating matters. Remote Sens. Environ. 280, 113188 https://doi.org/10.1016/j.rse.2022.113188.

Qi, L., Wang, M., Hu, C., 2023. Uncertainties in MODIS-derived *Ulva Prolifera* amounts in the Yellow Sea: a systematic evaluation using sentinel-2/MSI observations. IEEE Geosci. Remote Sens. Lett. 20, 1501805 https://doi.org/10.1109/LGRS.2023.3272889.

Ronneberger, O., Fischer, P., Brox, T., 2015. U-net: convolutional networks for biomedical image segmentation. In: Proceedings of the Medical Image Computing and Computer-Assisted Intervention–MICCAI 2015: 18th International Conference. Munich, Germany. October 5-9, 2015, Proceedings, Part III 18.

Rosenblatt, S.E., Wetmore, L.S., Anderson, T.W., 2022. Impacts of an invasive alga on recruitment of a temperate reef fish. J. Exp. Mar. Biol. Ecol. 551, 151733 https://doi.org/10.1016/j.jembe.2022.151733.

Shchepetkin, A.F., McWilliams, J.C., 2005. The regional oceanic modeling system (ROMS): a split-explicit, free-surface, topography-following-coordinate oceanic model. Ocean Model. 9 (4), 347–404.

Shin, J., Choi, J.G., Kim, S.H., Khim, B.K., Jo, Y.H., 2022. Environmental variables affecting Sargassum distribution in the East China Sea and the Yellow Sea. Front. Mar. Sci. 9 https://doi.org/10.3389/fmars.2022.1055339.

Su, L., Shan, T., Pang, S., Li, J., 2018. Analyses of the genetic structure of *Sargassum horneri* in the Yellow Sea: implications of the temporal and spatial relations among floating and benthic populations. J. Appl. Phycol. 30 (2), 1417–1424. https://doi.org/10.1007/s10811-017-1296-y.

Sun, J., Zhuang, D., 2009. Study on *Sargassum herneri* (Tarn) Ag around Nanji Islands. Mod. Fish. Inf. 24 (07), 25–28.

Umezaki, I., 1984. Ecological studies of *Sargassum horneri* (TURNER) C. AGARDH in Obama Bay, Japan Sea. Nippon Suisan Gakkaishi 50 (7), 1193–1200.

Wang, Z., Yuan, C., Zhang, X., Liu, Y., Fu, M., Xiao, J., 2023. Interannual variations of Sargassum blooms in the Yellow Sea and East China Sea during 2017–2021. Harmful Algae 126, 102451. https://doi.org/10.1016/j.hal.2023.102451.

Wu, R., Wu, H., Wang, Y., 2021. Modulation of shelf circulations under multiple river discharges in the East China Sea. J. Geophys. Res. Oceans 126 (4). https://doi.org/10.1029/2020JC016990 e2020JC016990.

Xiao, J., Fan, S., Wang, Z., Fu, M., Song, H., Wang, X., Yuan, C., Pang, M., Miao, X., Zhang, X., 2020. Decadal characteristics of the floating Ulva and Sargassum in the Subei Shoal, Yellow Sea. Acta Oceanol. Sin. 39 (10), 1–10.

Xing, Q., Guo, R., Wu, L., An, D., Cong, M., Qin, S., Li, X., 2017. High-resolution satellite observations of a new hazard of golden tides caused by floating Sargassum in winter in the Yellow Sea. IEEE Geosci. Remote Sens. Lett. 14 (10), 1815–1819. https://doi.org/10.1109/LGRS.2017.2737079.

Yu, J., Li, J., Wang, Q., Liu, Y., Gong, Q., 2019. Growth and resource accumulation of drifting Sargassum horneri (Fucales, Phaeophyta) in response to temperature and nitrogen supply. J. Ocean Univ. China 18, 1216. https://doi.org/10.1007/s11802-019-3835-4.

Yuan, C., Xiao, J., Zhang, X., Fu, M., Wang, Z., 2022. Two drifting paths of Sargassum bloom in the Yellow Sea and East China Sea during 2019–2020. Acta Oceanol. Sin. 41 (6), 78–87. https://doi.org/10.1007/s13131-021-1894-z.

Zhan, D., Liu, W., Xin, M., Wang, X., 2022. A preliminary study on origin of drifting *Sargassum horneri* in the North Yellow Sea. Trans. Oceanol. Limnol. 44 (04), 123–127 (in Chinese with English abstract).

Zhang, J., Ding, X., Zhuang, M., Wang, S., Chen, L., Shen, H., He, P., 2019. An increase in new Sargassum (Phaeophyceae) blooms along the coast of the East China Sea and Yellow Sea. Phycologia 58 (4), 374–381. https://doi.org/10.1080/00318884.2019.1585722.

Zhang, S., Hu, C., Barnes, B.B., Harrison, T.N., 2022. Monitoring Sargassum inundation on beaches and nearshore waters using planetscope/dove observations. IEEE Geosci. Remote Sens. Lett. 19, 1–5. https://doi.org/10.1109/LGRS.2022.3148684.

Zhang, Z., Liu, Q., Wang, Y., 2018. Road extraction by deep residual U-Net. IEEE Geosci. Remote Sens. Lett. 15 (5), 749–753.

Zhuang, M., Liu, J., Ding, X., He, J., Zhao, S., Wu, L., Gao, S., Zhao, C., Liu, D., Zhang, J., He, P., 2021. *Sargassum* blooms in the East China Sea and Yellow Sea: formation and management. Mar. Pollut. Bull. 162, 111845 https://doi.org/10.1016/j.marpolbul.2020.111845.

Zhuang, M., 2022. Molecular Biology Based Traceability Study of *Sargassum Horneri* Golden Tides in the Nearshore of China Doctoral dissertation. East China Normal University.